



Transition between Regular and Mach Reflections in Oblique Shock Wave-Oblique Detonation Wave Interactions

Xin HAN, Ruofan Qiu, Yancheng You3

Abstract

Standing oblique detonation engines (SODEs) have great potential in the field of air-breathing hypersonic propulsion, making it necessary to carry out an in-depth study of their key flow phenomena. In this paper, the asymmetric reflection of oblique detonation waves (ODWs) and oblique shock waves (OSWs) is investigated, and the transition mechanism between regular and Mach reflections is illustrated through theoretical analysis. In determining the reflection shock on the ODW side, two hypotheses, frozen chemistry and chemical equilibrium, are used to obtain two different sonic-point criteria, and the $RR \to MR$ transition occurs between these two criteria. The von Neumann criterion is derived based on the asymmetric reflection modeling of the leading inert shock of ODW and the OSW. The $MR \to RR$ transition point obtained through inviscid numerical simulation is slightly larger than this von Neumann criterion. This study provides a preliminary investigation of the complex ODW-OSW reflection phenomena in SODE combustors.

Keywords: OSW-ODW interactions, dual-solution, hysteresis, chemical non-equilibrium

Nomenclature

Latin

OSW – Oblique shock wave

ODW – Oblique detonation wave

SODE – Standing oblique detonation engine

RR – regular reflection MR – Mach reflection

ER - Equivalent Ratio

SSW – separation shock wave

RfSW - Reflected shock wave

Greek

 θ – wedge angle

 β – wavefront angle

Superscripts

fr – frozen chemistry

eq - chemical equilibrium

Subscripts

1 – upper wedge

2 - lower wedge

vN - the von Neumann condition

s_fr - the frozen chemistry sonic-point criterion

 $s_eq\ -\ the\ chemical\ equilibrium\ sonic-point\ crite-$

rion

e – equivalent

1. Introduction

In recent years, standing oblique detonation engines (SODEs) have received extensive attention in the field of air-breathing hypersonic propulsion[1, 2]. Zhang et al.[3] and Han et al.[4] reveal the flow structures in the combustor through large-scale SODE free-jet experiments conducted in a hypersonic shock tunnel, named JF-12. The shock-dominated flow is the main feature of the flow within this engine. The interaction between the shock wave and the detonation wave can be clearly observed in Fig. 1.

HiSST-2025-208
Transition between RR and MR in OSW-ODW interactions

¹School of Aerospace Engineering, Xiamen University, Xiamen 361005, China, hanxin@stu.xmu.edu.cn

²School of Aerospace Engineering, Xiamen University, Xiamen 361005, China, rf_qiu@xmu.edu.cn ³School of Aerospace Engineering, Xiamen University, Xiamen 361005, China, yancheng.you@xmu.edu.cn

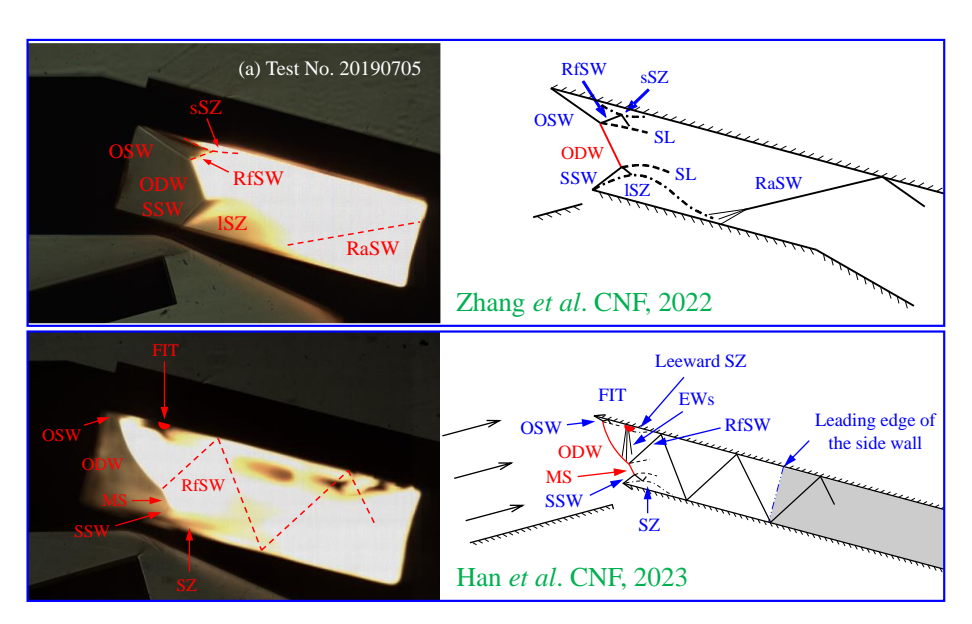


Fig 1. Schlieren photographs and schematics of SODE combustor flow fields.

The reflection of detonation waves is a common phenomenon during their propagation. Many experiments and numerical simulations have focused on the unsteady reflection, i.e., the interaction between a moving detonation wave and a fixed wedge. However, what is commonly observed in combustors is the phenomenon of steady reflection of the detonation wave. In SODE combustors, the interaction of the ODW with the turbulent boundary layer induces flow separation, during which the separation shock wave (SSW) interacts with the incident ODW to form either a regular or Mach reflection wave structure. It is worth noting that in both experimental tests and numerical simulations, the SSW is often treated as an inert OSW, which can be attributed to the following three reasons:

(1). In the turbulent boundary layer separation, the SSW is relatively weak, making it generally more difficult to induce the formation of detonation waves. (2). In SODE combustors, techniques such as expansion walls and boundary layer control methods (e.g., blowing/bleeding) are employed to further attenuate the SSW. (3). SODEs use intrusive fuel injection methods, such as strut injections and cantilevered ramps, which reduce the fuel content near the wall surface, leaving the SSW front in a lean combustion state. This is unfavorable for the transformation of the SSW into a detonation wave.

Therefore, in this paper, the issue of interactions between SSW and incident ODW is reduced to the problem of the asymmetric reflection of OSW and ODW in steady flows, with the physical model and computational domain depicted in Fig. 2. The numerical methods and code validation are presented in Section 2. The mechanisms of the transition between regular and Mach reflection are then analyzed, followed by the presentation of the dual-solution domain. Finally, the hysteresis phenomenon in asymmetric reflection is discussed.

2. Numerical details

In this paper, the governing equations, multispecies reactive Euler equations, are solved by the cell-centroidal finite volume method. For inviscid fluxes, these interface values are reconstructed using the second-order total variation diminishing (TVD) scheme with the Continuous limiter, and the Harten-Lax-van Leer contact (HLLC) approximate Riemann solver is used to solve the numerical flux. The second-order implicit scheme is used for time integration. The operator-splitting method is used to overcome the stiffness problem of the source term, where each flow step advances a four-step chemical reaction, and the differential equation of chemical reaction part is solved by a point-implicit method. The source term of chemical reactions is calculated using a detailed hydrogen-air combustion mechanism (involving 19 reversible elementary reactions among 9 species)[5, 6], which is widely used in the numerical simulations

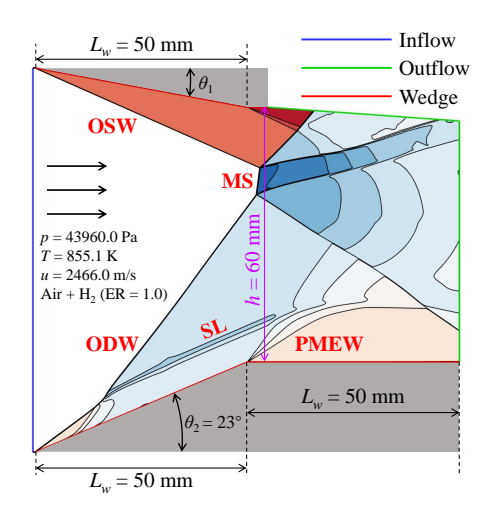


Fig 2. Detailed geometry of the computational domain.

of oblique detonation. More numerical details and some validation examples can also be found in Han et al.[7]. To validate the accuracy of the numerical method with the chemical reaction mechanism, a numerical validation of the detonation wave reflection experiment is given in this paper. The experimental conditions are described with reference to Ref.[8]. The numerical simulations closely match the wave structures of the Mach reflection and the regular reflection, as shown in Fig. 3. The χ in the experiment in Fig. 3(a) is 6°, and the χ obtained from the numerical simulation is also 6°.

3. The $RR \rightarrow MR$ transition

The detonation/shock polar analysis for the asymmetric OSW-ODW reflection in steady flow is presented in Fig. 4. In this analysis, R1 and R2 represent the polar diagrams of the OSW and ODW in the free-stream, respectively. Due to the high temperature of the free-stream, the assumption of a calorically perfect gas becomes invalid, and vibrational energy excitation must be considered. As a result, the polar diagram R1 is derived by incorporating vibrational excitation into the shock relations. The polar diagram R2 for the ODW is obtained by solving the shock relations coupled with chemical equilibrium. Two reflection shock waves are generated in the asymmetric OSW-ODW reflection flow field, as shown in Fig. 5. The reflection shock wave on the OSW side is denoted as RfSW2, while the reflection shock wave on the ODW side is denoted as RfSW1. The RfSW2 is a detonation wave, and its polar diagram is determined using shock relations coupled with chemical equilibrium.

In the OSW-ODW reflection problem discussed in this paper, the key challenge is determining the polar diagram of RfSW1. The deflection angle of the free-stream across the ODW is 23°, with theoretical values for the post-wave temperature and Mach number of 3076.9 K and 1.44, respectively. Given the high temperature of the gas mixture, vibration excitation must be considered in the reflection process. By solving the shock relations with only considering vibration excitation, and assuming the chemical kinetic process is frozen (i.e., maintaining a constant species composition when the flow across the RfSW1), the polar diagram r^{fr} is derived. Since the reversible nature of the chemical kinetic model employed in this paper, incompletely reacted hydrogen and intermediate species (e.g., H, O, OH, etc.) are observed behind the detonation wave. As the gas mixture passes through the reflected shock, its temperature increases, causing the chemical equilibrium to shift in the reverse direction, which results in a higher mass fraction of hydrogen. Under the hypothesis that the gas mixture remains in chemical equilibrium after passing through the RfSW1, the polar diagram r^{eq} can be obtained by solving the shock relations coupled with chemical equilibrium. As shown in Fig. 4, the difference between the two polar

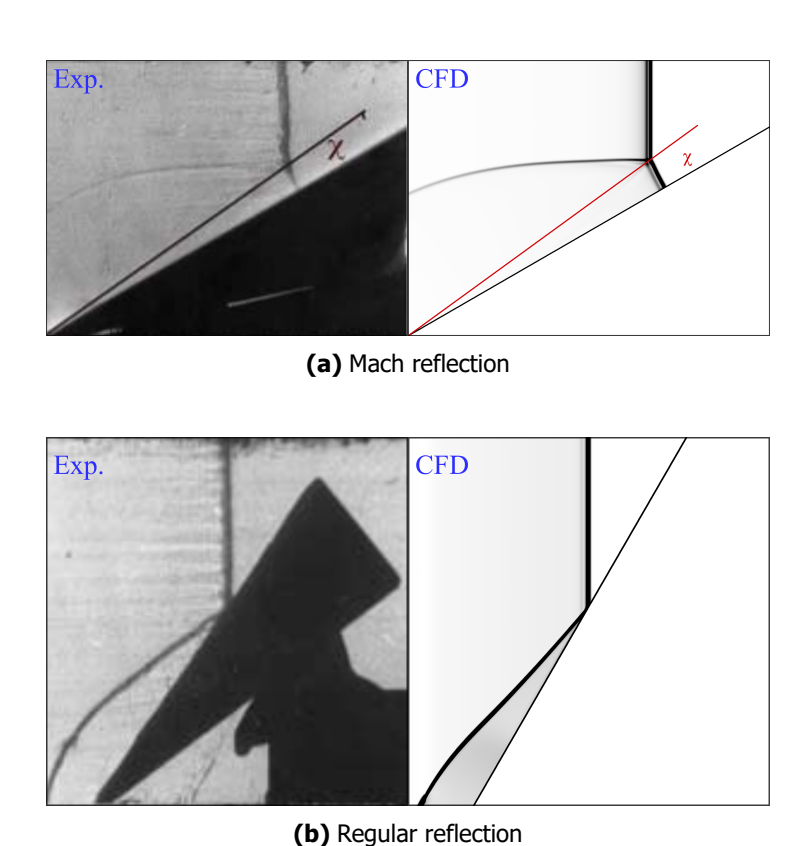


Fig 3. Comparison between experiment and numerical schlieren.

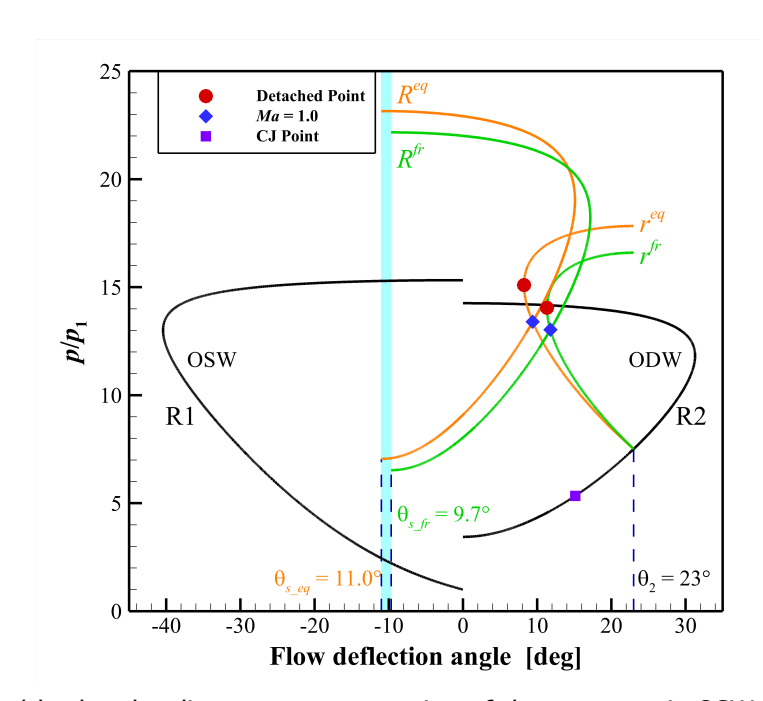


Fig 4. Detonation/shock polar diagrams representation of the asymmetric OSW-ODW reflection in a steady flow field.

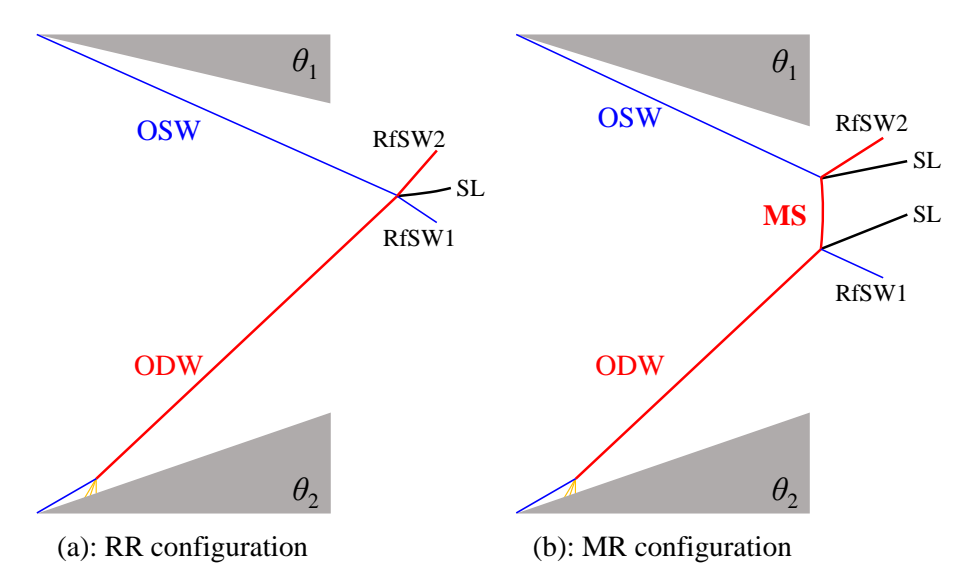


Fig 5. Schematic illustration of (a) a RR wave configuration and (b) a MR wave configuration in steady flows.

diagrams is quite evident.

In this paper, the sonic criterion is adopted as the critical criterion for the transition from regular to Mach reflection. Due to the different hypotheses regarding the state of gas mixture behind the RfSW1 (frozen chemistry versus chemical equilibrium), the sonic points on the two polar diagrams are distinct, as shown in Fig. 4. Consequently, two distinct critical criteria are established: the equilibrium sonic criterion, denoted as θ_{s_eq} , and the frozen sonic criterion, denoted as θ_{s_fr} . Numerical simulations indicate that the transition point from regular to Mach reflection lies between the equilibrium and frozen sonic criteria. This outcome is expected, as the actual flow exhibits chemical non-equilibrium, and the numerical simulations in this paper also employ a finite-rate chemical model. Therefore, chemical equilibrium and frozen chemistry represent two limiting hypotheses.

4. The $MR \rightarrow RR$ transition

At the same flow deflection angle, the higher temperature behind the ODW results in a lower post-wave Mach number compared to that behind the OSW. The pressure increase caused by the reflection shock on the ODW side is smaller, and the weak solution branches of the reflection shock (i.e., r^{fr} or r^{eq}) do not intersect with the strong solution branches of R1 and R2. The polar diagram (Fig. 4) indicates that there does not appear to be a von Neumann condition in the asymmetric reflection for OSW and ODW under the current inflow, i.e., there is no dual-solution domain. However, in the polar diagrams, the shock/detonation waves are treated as discontinuities. The detonation wave is generally regarded as the leading shock and the subsequent reaction surface, which are not fully coupled due to chemical non-equilibrium, as shown in Fig. 6.

In the asymmetric reflection of OSW and ODW, OSW first interacts with the inert shock. If OSW interacts with the inert shock and forms Mach reflection, then Mach reflection can be induced throughout the entire OSW-ODW asymmetric reflection flow field. For $\theta_2=23^\circ$, the wavefront angle of the ODW is 53.4°, which is the same as that of the inert shock. The inert shock is equivalent to the shock wave generated by a wedge with an angle of 35.6°(i.e., θ_e) under the current inflow condition (frozen chemistry). The polar analysis of the asymmetric reflection between the OSW and the inert shock is shown in Fig. 7. A von Neumann criterion exists in the reflection of the OSW and inert shock, which implies the existence of a dual-solution domain in the asymmetric reflection of OSW and ODW.

Inviscid numerical simulations are used to determine the transition points of $RR \longleftrightarrow MR$, with the flow

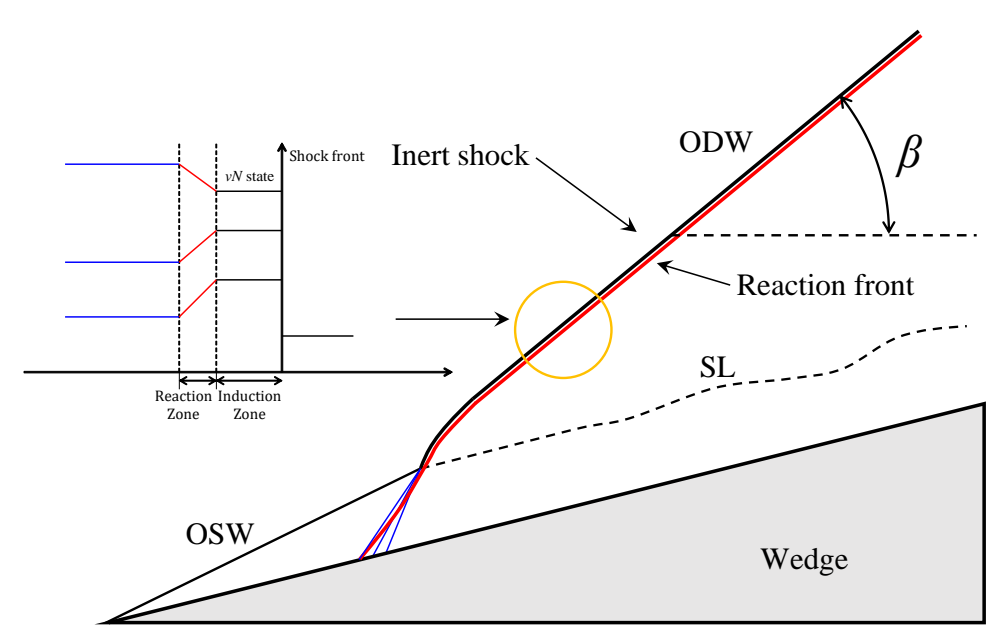


Fig 6. Schematic of a typical ODW.

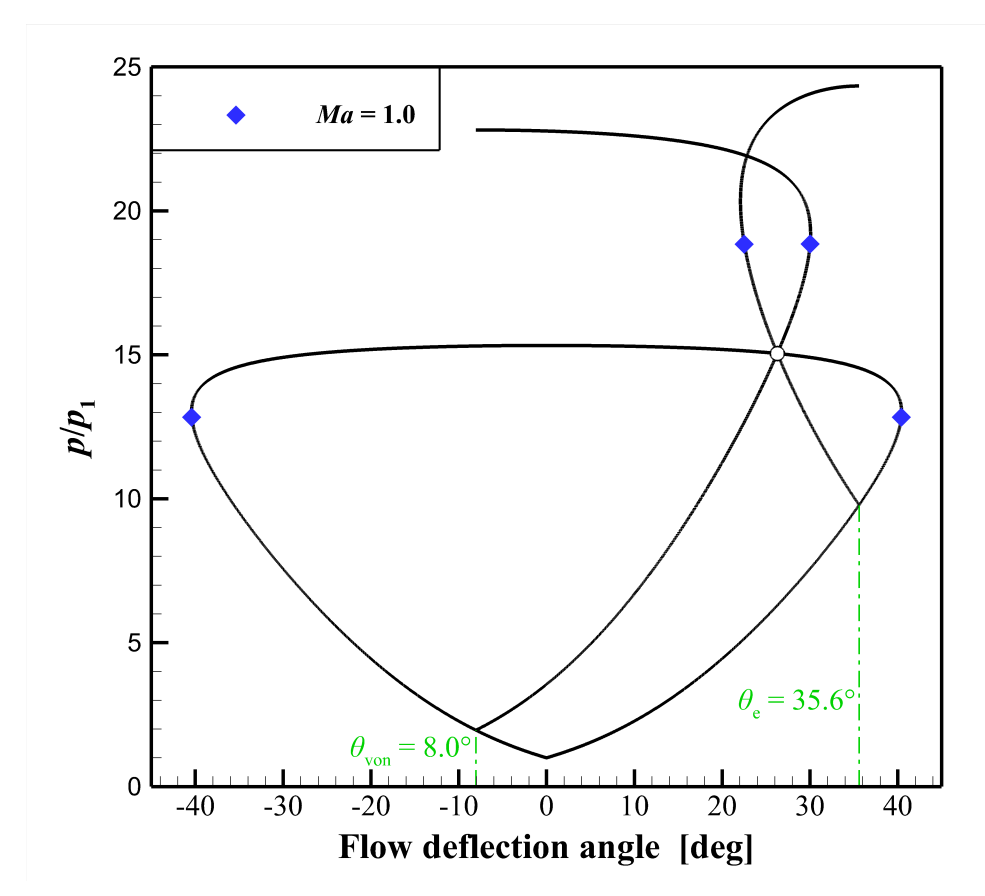


Fig 7. Pressure-deflection polars illustrating the von Neumann condition in the reflection of the inert shock and the OSW.

deflection angle θ_1 varied in intervals of 0.1°. The $RR \to MR$ transition point is numerically determined to be 10.25°, and the $MR \to RR$ transition point is 8.45°, with the interval [8.5°, 10.2°] representing the dual-solution domain. As shown in Fig. 8, the $RR \to MR$ transition point lies between θ_{s_fr} and θ_{s_eq} , while the $MR \to RR$ transition point slightly greater than the von Neumann criterion of the asymmetric reflection between OSW and inert shock.

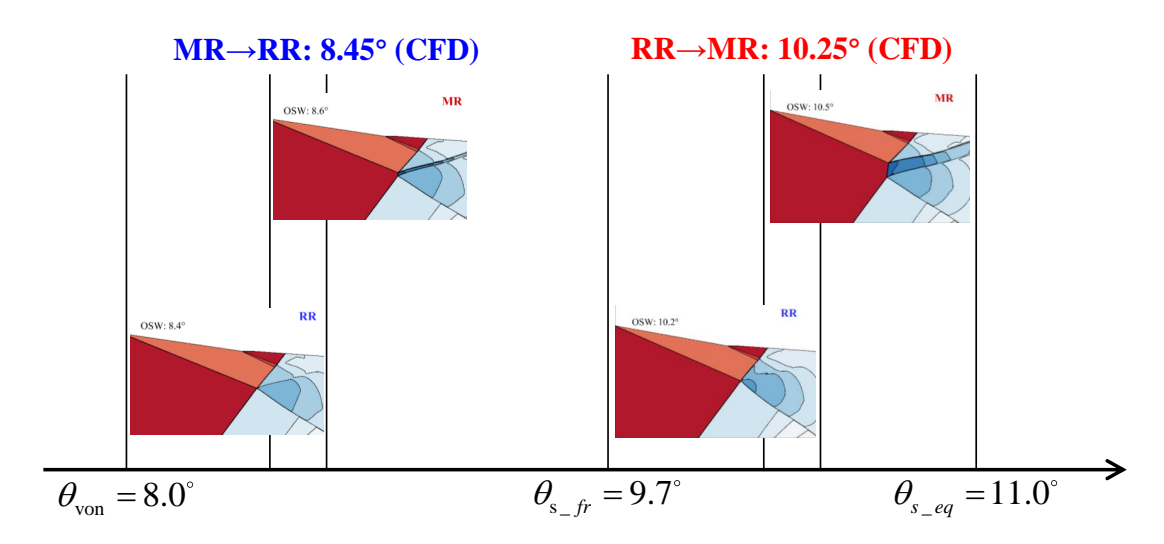


Fig 8. Comparison among the analytical $RR \longleftrightarrow MR$ transition points and CFD results.

5. The hysteresis loop

With θ_2 fixed at 23°, θ_1 follows a variation path: $8.4^\circ \rightarrow 8.6^\circ \rightarrow 10.2^\circ \rightarrow 10.5^\circ \rightarrow 10.2^\circ \rightarrow 8.6^\circ \rightarrow 8.4^\circ$, and the corresponding evolution of the flow field illustrated in Fig. 9. For clarity in the discussion, the path $8.4^\circ \rightarrow 8.6^\circ \rightarrow 10.2^\circ \rightarrow 10.5^\circ$, which corresponds to an increase in θ_1 , is defined as the positive path, while the path $10.5^\circ \rightarrow 10.2^\circ \rightarrow 8.6^\circ \rightarrow 8.4^\circ$, corresponding to a decrease in θ_1 , is defined as the negative path. Using the quasi-stationary technique[9], the converged flow field from the previous geometric configuration is used as the initial condition for the subsequent case involving variations in θ_1 . Along the positive path, when θ_1 lies in the closed interval [8.4°, 10.2°], the flow field exhibits a regular reflection wave configuration. However, as θ_1 increases from 10.2°to 10.5°, the reflection pattern formed by OSW and ODW transitions from regular reflection to Mach reflection. Along the negative path, the flow field remains in the Mach reflection wave configuration as θ_1 decreases from 10.5°to 8.6°. However, as θ_1 decreases further from 8.6°to 8.4°, the Mach stem within the flow field disappears, and the flow field transitions to a regular reflection wave configuration. In the numerical simulations in this section, the angular interval [8.6°, 10.2°] of θ_1 represents the dual-solution domain, where the reflection pattern depends on the evolutionary path.

6. Conclusion

In this paper, the asymmetric reflection of ODW and OSW is investigated through numerical simulation and theoretical analysis, and the mechanism of RR and MR transition is presented. For the $RR \to MR$ transition, the core is to determine the polar of RfSW1 (see Fig. 5). By using two hypotheses of frozen chemistry and chemical equilibrium, two different sonic-point criteria are obtained, and the $RR \to MR$ transition occurs between these two sonic-point criteria. It is easy to understand that the actual physicochemical processes are chemical non-equilibrium and the chemical kinetic model used in this paper is also a finite-rate model. For the $MR \to RR$ transition point, the core is the interference of the leading inert shock of the ODW with the OSW. The $MR \to RR$ von Neumann condition is obtained by modeling the asymmetric reflection of OSW with inert shock. Numerical simulations show that in the asymmetric reflection of ODW with OSW. the transition point of $MR \to RR$ is slightly larger than

this von Neumann criterion. The hysteresis loop of the flow field evolution is obtained through inviscid numerical simulation, which verifies the reasonableness of the transition mechanism derived from the theoretical analysis.

Under the current inflow condition, a dual-solution domain exists for the asymmetric reflection of ODW and OSW. This dual-solution domain cannot be directly obtained by polar analysis of ODW and OSW (see Fig. 4), which highlights the complexity of the interaction between ODW and OSW.

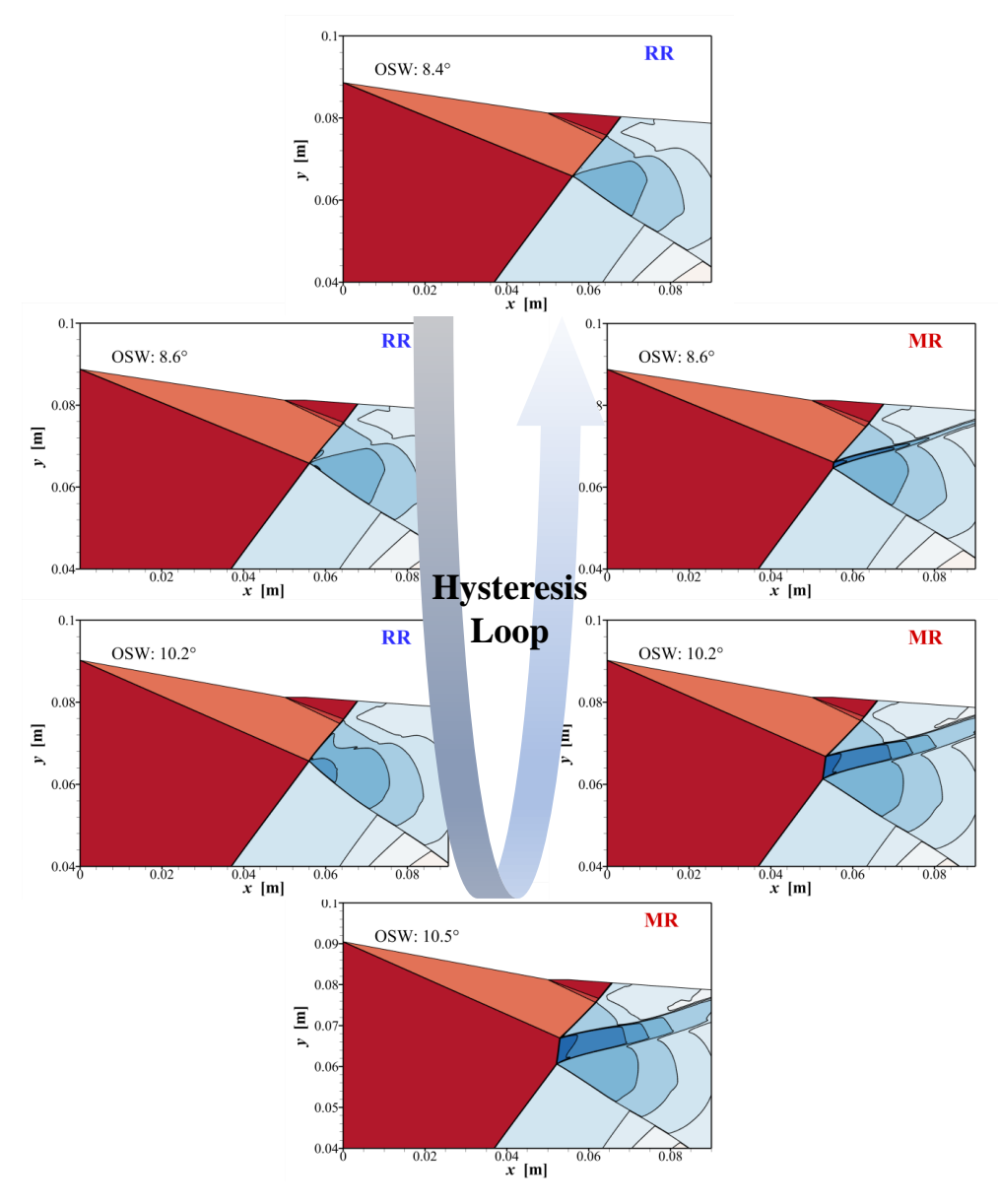


Fig 9. Mach contours illustrating the hysteresis loop.

References

[1] D.A. Rosato, M. Thornton, J. Sosa, C. Bachman, G.B. Goodwin, and K.A. Ahmed. Stabilized detonation for hypersonic propulsion. *Proc. Natl. Acad. Sci. U.S.A.*, 118(20):e2102244118, 2021.

- [2] Z. Jiang. Standing oblique detonation for hypersonic propulsion: A review. *Prog. Aerosp. Sci.*, 143:100955, 2023.
- [3] Z. Zhang, C. Wen, C. Yuan, Y. Liu, G. Han, C. Wang, and Z. Jiang. An experimental study of formation of stabilized oblique detonation waves in a combustor. *Combust. Flame*, 237:111868, 2022.
- [4] X. Han, Y. Liu, Z. Zhang, W. Zhang, C. Yuan, G. Han, and Z. Jiang. Experimental demonstration of forced initiation of kerosene oblique detonation by an on-wedge trip in an ode model. *Combust. Flame*, 258:113102, 2023.
- [5] C.J. Jachimowski. An analytical study of the hydrogen-air reaction mechanism with application to scramjet combustion. Technical Report 2791, Langley Research Center, 1988. NASA Technical Paper.
- [6] G.J. Wilson and R.W. MacCormack. Modeling supersonic combustion using a fully implicit numerical method. *AIAA J.*, 30(4):1008–1015, 1992.
- [7] X. Han, R. Qiu, and Y. You. Hysteresis phenomenon in oblique detonation wave/boundary layer interactions. *Combust. Flame*, 281:114399, 2025.
- [8] G.O. Thomas and R.Ll. Williams. Detonation interaction with wedges and bends. *Shock waves*, 11(6):481–492, 2002.
- [9] M.S. Ivanov, G. Ben-Dor, T. Elperin, A.N. Kudryavtsev, and D.V. Khotyanovsky. The reflection of asymmetric shock waves in steady flows: a numerical investigation. *J. Fluid Mech.*, 469:71–87, 2002.